

1

2

Geophysical Research Letters

3

Supporting Information for

4

Observations and Modeling of a Hydrothermal Plume in Yellowstone Lake

5

Robert A. Sohn¹, Karen Luttrell², Emily Shroyer³, Christian Stranne⁴, Robert N. Harris³, and
6 Julia E. Favorito³

6

7

¹Woods Hole Oceanographic Institution, Woods Hole, MA, 02543.

8

²Louisiana State University, Baton Rouge, LA.

9

³Oregon State University, Corvallis, OR.

10

⁴Stockholm University, Sweden

11

12 **Contents of this file**

13

14

Text S1- S2

15

Figures S1-S5

16

17

Introduction

18

This supporting information provides additional details regarding the Acoustic-Doppler-
19 Current-Profiler data (Text S1) and a description of sensitivity tests conducted to assess
20 the impact of our modeling assumptions on our results (Text S2).

21

Text S1.

22

Acoustic-Doppler-Current-Profiler (ADCP) surveys

23

The ADCP data were collected using a downward-looking 300 kHz *RDI Navigator*
24 system mounted on a pole rigidly affixed to *R/V Annie II*. The data were acquired when
25 the research vessel was stationary or moving very slowly (< 4 knots) over the Deep Hole
26 hydrothermal site. The transducer was mounted roughly 2 m beneath the surface,
27 allowing for resolution of currents from ~ 6 m beneath the surface to within ~15 m of
28 the bottom. The maximum measured range between the transducer and the bottom was
29 95 m; current measurements in the lower 15% of the range were removed to avoid side-
30 lobe contamination. Currents were sampled in 4 m vertical bins averaged into 2-minute

31 ensembles. Flagging of data (correlation threshold of 64) and conversion from beam to
32 earth coordinates was done internally by the ADCP prior to ensemble averaging. The
33 ADCP maintained bottom-tracking throughout the deployment, so that removal of ship
34 motion to retrieve water column velocity was straightforward. Time ensembles were
35 mapped to GPS latitude and longitude through a linear interpolation of GPS time onto
36 ADCP time.

37 ADCP data were acquired during two discrete survey periods: a 4-hour window on
38 13 August and a 5-hour window on 14 August. The two surveys were separated from one
39 another by roughly 12 hours. The entire survey on 13 August was opportunistic - i.e.,
40 data were acquired while the research vessel was conducting other research - and the
41 survey pattern was therefore not optimized for plume measurements. The survey on 14
42 August was conducted in two parts. For the first ~3 hours, data was collected in a similar,
43 opportunistic way, but for the final ~2 hours the survey pattern was expressly designed
44 to systematically measure currents in the water column above the Deep Hole
45 hydrothermal field (radiator survey grid pattern shown in Figure 1b).

46 The systematic survey on 14 August provides an opportunity to assess the spatial
47 structure of the water column plume above the hydrothermal field. The vertical velocity
48 field is described in the main body of the manuscript. The horizontal velocity field is
49 more complex than the vertical velocity field, with significant spatio-temporal variability,
50 and with current direction varying as a function of depth (Figure S1). Unfortunately, the
51 sampling was too slow (2-minute ensemble averages) to resolve motions at the local
52 buoyancy period of the thermocline (~2.5 min), and likely aliased large-scale motions
53 associated with seiching (78 min fundamental mode compared to ~2 hour survey
54 duration). The background current field into which the plume fluids rise is not adequately
55 constrained by our data. Streamline plots (Figure S2) provide a sense of the complex
56 interaction between the buoyant plume and the ambient current field.

57 The processed ADCP data are available for download as *Matlab* files from Sohn et
58 al., (2019a), doi: 10.1594/IEDA/324712.

59

60 **Text S2**

61 Numerical model sensitivity tests

62 Our model makes assumptions about the nature of hydrothermal discharge at the lake
63 floor that may affect our results. We conducted sensitivity tests to assess the impact of
64 these assumptions on our analyses, and report those results here (Figure S3).

65

66 First, we consider the assumption that hydrothermal discharge occurs through a single
67 feature at the bottom boundary (i.e., the lake floor), of a fixed size. By contrast, visual
68 observations from ROV dives have established that discharge at the Deep Hole site
69 occurs through numerous small features that are distributed over a wider area. Our
70 baseline model assumes that discharge occurs evenly over an area of 54,000 m², which
71 spans the entire pockmark field at the Deep Hole site. To understand how this
72 assumption affects our results we ran the model with initial discharge areas at the
73 bottom boundary ranging from 54 to 54,000 m². The results demonstrate that variations

74 in the source area have a weak and essentially negligible effect on all model parameters
75 except for boundary velocity (Figure S3b). Variations in source area are almost exactly
76 balanced by variations in the boundary velocity such that the total mass, heat and
77 buoyancy fluxes of the best-fitting model parameters do not change.

78

79 Second, we consider the source depth assumption. The model assumes that fluid
80 discharge occurs at a single depth, whereas the various discrete venting sites in the
81 pockmark field sampled during HD-YLAKE fieldwork have depths that vary by ~8 m (109-
82 117 m). Although this depth variation is not large, it nevertheless has a significant impact
83 on the flux estimates for the best-fitting model (Figure S3d). This high degree of
84 sensitivity is expected because changing the source depth changes the neutral buoyancy
85 height estimate by an equal amount, and the plume fluxes in the best-fitting model are
86 primarily constrained by the height of the neutral buoyancy horizon about the source.
87 Changing the source depth boundary condition by ± 5 m changes the best-fitting plume
88 heat flux by ± 7 MW.

89

90 We did not use the fluid temperature anomaly at the plume neutral height to constrain
91 the model, but our simulations were able to reproduce the anomaly to within $\sim 0.01^\circ\text{C}$
92 (Figure S3c). The initial plume fluid temperature at the lake floor boundary for all of our
93 best-fitting simulations is within a relatively narrow range (~ 9.1 - 9.7°C), regardless of the
94 assumed source depth and area (Figure S3a).

95

96 We did not use the vertical velocities observed during the ADCP surveys to formally
97 constrain the modeling results, but we can nevertheless compare the vertical velocity
98 profile from the model output to the observed profiles to assess the model accuracy
99 (Figure S4). As described in the main text body, the positive vertical velocities observed
100 in the upper part of the water column above the thermocline on 13 August (see main
101 text Figure 3a) are not explained by our model and are likely due to other hydrodynamic
102 processes. Below the thermocline, however, our model matches the observed 1D vertical
103 velocity profile observed over the Deep Hole site fairly well.

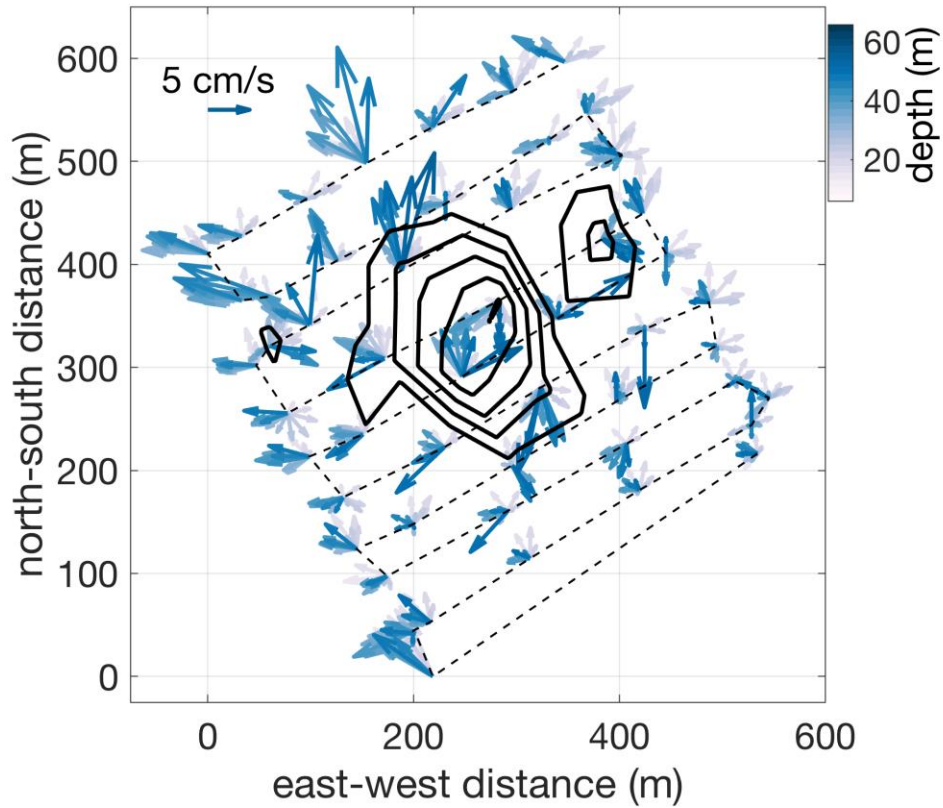
104

105 In summary, our model is primarily sensitive to assumptions regarding the source depth
106 through its impact on the plume's neutral height (since the depth horizon of the neutral
107 layer is fixed by observations, variations in source depth translate directly into variations
108 in neutral height). The assumed source area at the bottom boundary has a negligible
109 impact on the results because the model adjusts the fluid velocity at the bottom
110 boundary so that the total flux required to match the neutral height observed is
111 preserved. Although the observed temperature anomaly at the plume neutral height and
112 the vertical velocity profiles were not used to constrain the model, the model results
113 nevertheless reproduce these parameters satisfactorily.

114

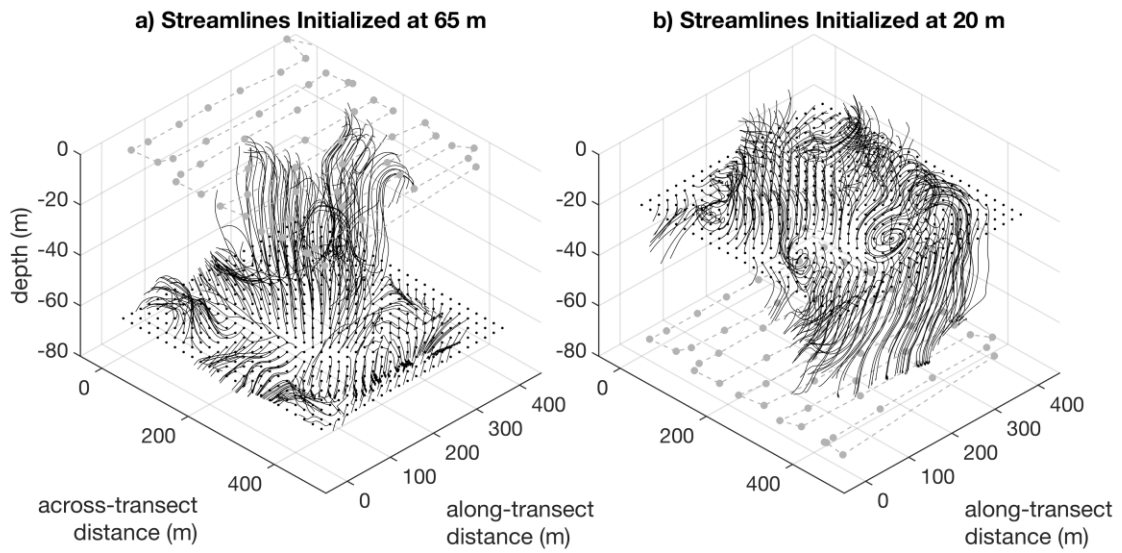
115 The sensitivity of the model to the plume neutral height estimate is expected given the
116 relationship between buoyancy flux and neutral height in Equation 1 of the text, which is
117 scaled by the buoyancy frequency of the ambient medium. Our estimate buoyancy

118 frequency depends on the interval over which it is calculated because of the strong
119 density gradient in the thermocline (Figure S5). We find that the buoyancy flux from our
120 baseline numerical model is reproduced in Equation 1 if the buoyancy frequency is
121 calculated over the interval from the source depth at 115 m to 25 m.
122



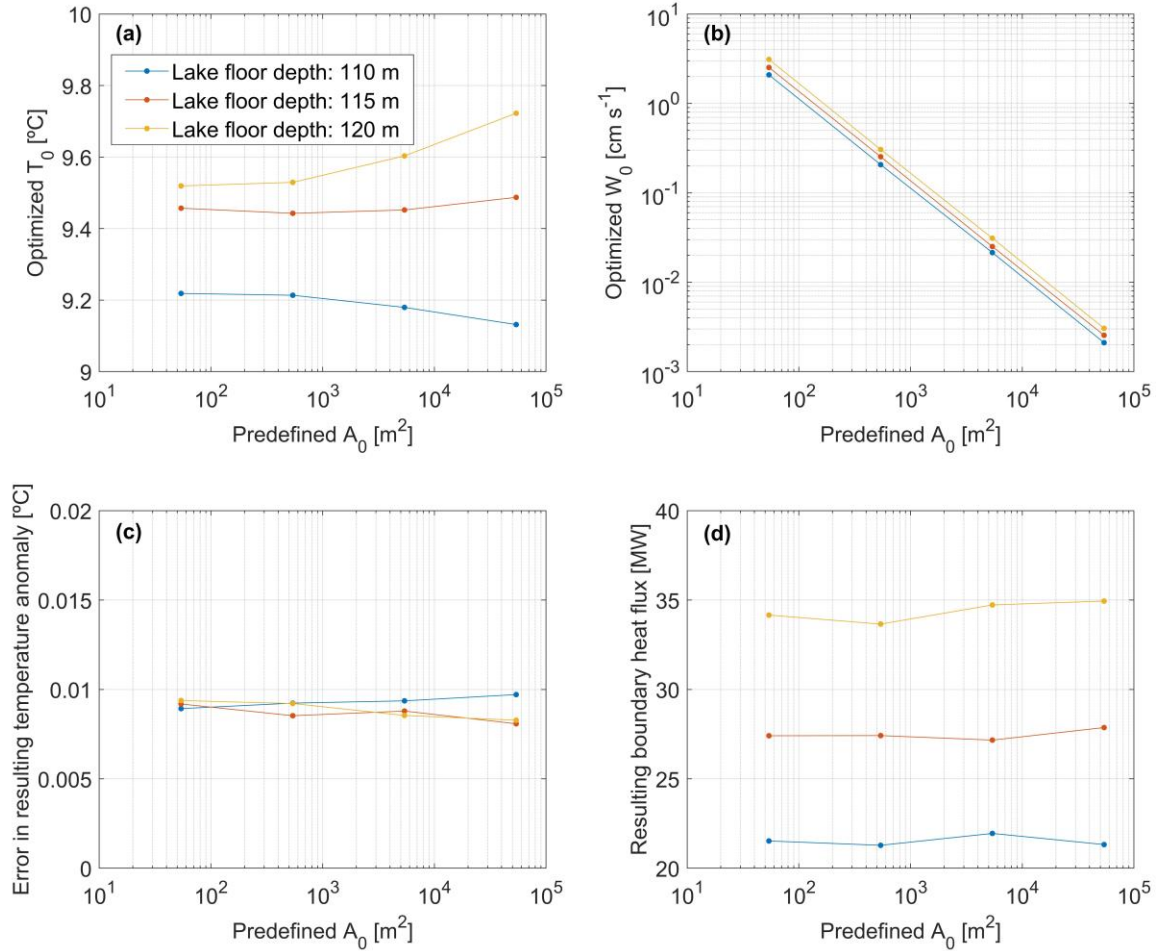
123
124
125
126
127
128
129
130
131

Figure S1. Horizontal velocity as a function of depth measured during the radiator survey on 14 August, 2018. Vectors are shown for each two-minute ensemble average. The duration of the radiator survey was roughly the length of the dominant seiche period. The measured flow field is complex. A general tendency for flow away from the region of upwelling is evident, as is significant vertical shear. Contours show the depth mean vertical velocity at 1 cm s^{-1} intervals in regions of upwelling.



132

133 **Figure S2.** Streamlines calculated from 4-m gridded radiator survey data. Streamlines
 134 are initialized at 65 m (left) and 20 m (right) depth at 20-m intervals in the horizontal.
 135 The ship track and ADCP ensembles are shown in grey. The integration step is taken
 136 over 1 m and continued for 100 intervals. Streamlines highlight the tendency for upward
 137 (downward) motions near (away from) the plume centerline, as well as the similarity in
 138 the magnitude of horizontal and vertical velocity.



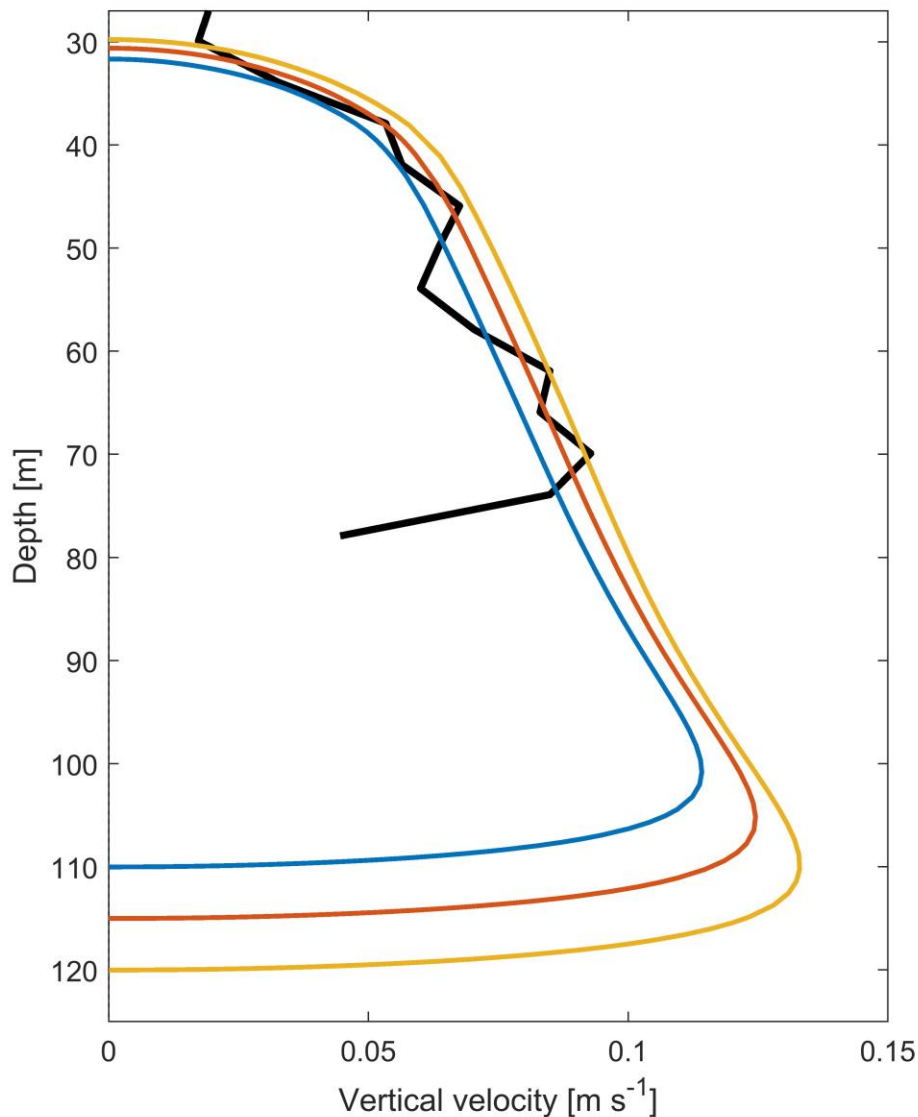
139

140 **Figure S3.** Sensitivity tests for boundary source area and depth. Optimized boundary
 141 temperature (a) and vertical velocity (b) for different predefined boundary areas and
 142 lake floor depths. c) Error in resulting temperature anomaly (compared to CTD data) and
 143 (d) resulting heat flux for different predefined boundary areas and lake floor depths.

144

145

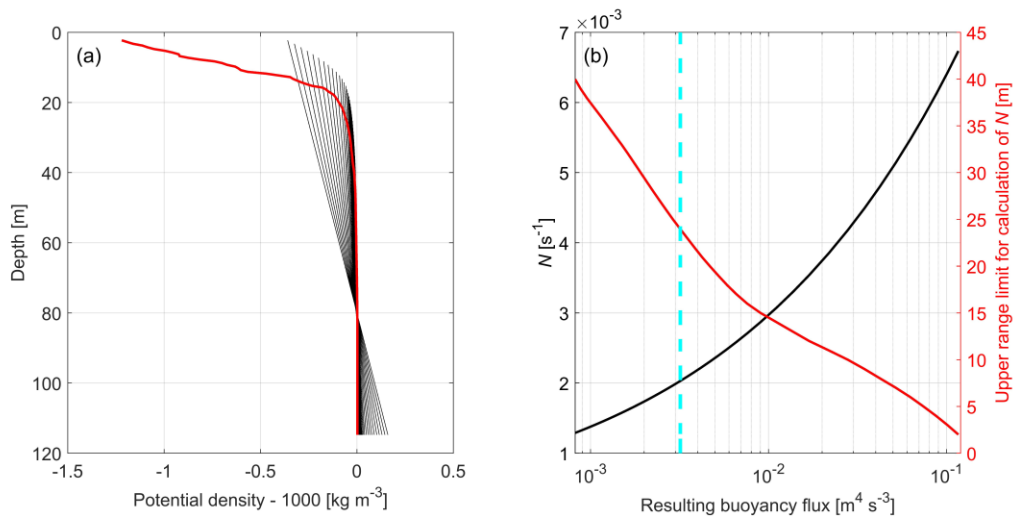
146



147

148 **Figure S4.** Comparison of 1D average vertical velocity profile from Deep Hole site (black)
 149 with resulting vertical velocity profiles from best-fitting numerical models for three
 150 different source depths (blue: 110 m, red: 115 m and yellow: 120 m). The modeled
 151 profiles represent values averaged over the radius of the buoyant plume as it rises
 152 through the water column. The 1D average profile from the ADCP surveys only extends
 153 to a depth of ~80 m because deeper intervals were truncated to avoid side-lobe
 154 contamination due to beam spreading. In both the observed and modeled profiles
 155 positive vertical velocities extend slightly above the plume's neutral depth (45 m),
 156 reflecting the overshoot expected for these features. Over the depth interval with robust
 157 estimates for the average vertical velocity (~30-80 m) the model output agrees fairly well

158 with the observations regardless of the source depth estimate, but the baseline estimate
159 of 115 m matches the observed profile best.



160

161 Figure S5. a) Observed background potential density (red line, reproduced from Fig. 2c in
162 the main text) and linear regressions between the lake floor at 120 m depth and an
163 upper limit ranging between 2 to 40 m below the lake surface (black lines). b) Resulting
164 buoyancy flux (x-axis) as a function of the Brunt-Vaisalla (buoyancy) frequency (black)
165 and the corresponding range over which the Brunt-Vaisalla frequency is calculated (red).
166 The buoyancy flux from the best-fitting numerical plume model ($3.2 \times 10^{-3} \text{ m}^4 \text{ s}^{-3}$) is
167 marked with a cyan line.